ISBN: 978-3-95450-248-6 ISSN: 2673-5490 doi: 10.18429/JACoW-IPAC2025-MOPB035

# TOWARDS GAMMA-RAY FREE-ELECTRON LASERS

A. Mak*, N. R. Thompson
STFC Daresbury Laboratory & The Cockcroft Institute, Warrington, United Kingdom



*Abstract*

The free-electron laser (FEL), powered by an accelerator and equipped with an undulator, produces intense coherent radiation at ever-shorter wavelengths. Whilst the hard x-ray regime represents the current state of the art, the gamma-ray regime remains the next objective. Gamma-ray lasers, deemed one of the most profound and intriguing challenges in physics by the 2003 Nobel Laureate, hold the key to unlocking the largely unexplored nuclear domain. This article introduces a novel scheme that harnesses FEL harmonics, offering a pathway for existing x-ray FELs to operate as gamma-ray lasers.

## INTRODUCTION

The free-electron laser (FEL) has proven its capability to generate coherent radiation at extremely short wavelengths. FEL facilities such as the European XFEL [1], LCLS [2], PAL XFEL [3], SACLA [4], and SwissFEL [5] routinely operate in the hard x-ray regime, providing the precision needed to probe atomic and molecular structures [6, 7].

Beyond the hard x-ray regime, the gamma-ray (or $\gamma$-ray) regime represents the next frontier for FELs, characterised by photon energies above 100 keV and wavelengths below 10 picometres (pm). This regime is pivotal to the burgeoning field of nuclear photonics [8, 9]. In his 2003 Nobel Lecture, Vitaly Ginzburg identified $\gamma$-ray lasers as amongst the 30 most "important and interesting" problems in physics [10].

Harmonic lasing [11, 12] offers a viable avenue towards this objective. By utilising the $h^{\text{th}}$ harmonic instead of the fundamental, the minimum attainable wavelength scales down by a factor of $h$ for a given electron beam energy and undulator tuning range. This could extend the spectral reach of existing x-ray FELs into the $\gamma$-ray regime without major infrastructure upgrades.

The efficacy of harmonic lasing can be characterised by two metrics: (i) the brightness of the target harmonic and (ii) the signal-to-noise ratio (SNR). In conventional self-amplified spontaneous emission (SASE), the fundamental typically dominates over higher harmonics in both power and brightness, resulting in a suboptimal SNR.

A phase shifter scheme [11] was previously proposed to suppress the fundamental whilst preserving gain at the target harmonic. However, its effectiveness is limited in the absence of an external seed [12]. To address this challenge, a novel split-undulator scheme is proposed in this article.

Other schemes for harmonic generation exist, such as HGHG [13], EEHG [14], PEHG [15] and HLSS [16]. Yet, they require the target wavelength $\lambda_{\text{tar}}$ to be the fundamental resonant wavelength $\lambda_{\text{res}}$ within specific undulator sections. As such, they are less suited for the purpose of extending the spectral reach for a given undulator tuning range. In addition, most rely on external laser systems for electron beam modulation, thereby increasing system complexity.

This work forms part of the research and development effort within the UK XFEL Conceptual Design and Options Analysis project [17], aimed at delivering a next-generation FEL facility for scientific and industrial applications.

* Corresponding author: Alan Mak, alan.mak@stfc.ac.uk

## METHOD

### *Case Definition*

This study aims to compare and contrast three schemes using the simulation code GENESIS 1.3 (version 4) [18]. All the simulations are performed for the same case, which is based on the SASE1 line of the European XFEL [19, 20] and has the electron beam parameters shown in Table 1.

Table 1: Electron Beam Parameters in the Simulations

| Parameter | Symbol | Value |
|---|---|---|
| Beam energy | $\gamma m_e c^2$ | 17.5 GeV |
| Relative energy spread | $\sigma_\gamma/\gamma$ | $2.34 \times 10^{-4}$ |
| Peak current | $I_0$ | 4.5 kA |
| Bunch charge | $Q$ | 20 pC |
| Normalised emittance | $\gamma\epsilon_{x,y}$ | 0.32 mm mrad |
| Average radius | $\bar{\sigma}_{x,y}$ | 17 µm |

The simulated FEL line comprises 36 planar undulator segments interleaved with drift spaces. Each segment has length 5 m and each drift space 1.1 m. The $K$ parameters of the segments are independently adjustable, whilst the undulator period $\lambda_u$ is fixed at 40 mm throughout.

Each drift space incorporates a quadrupole magnet and a phase shifter. The quadrupoles form a FODO lattice that provides the transverse focusing necessary for the electron beam to maintain the average radius shown in Table 1.

### *Harmonic Lasing*

The target wavelength $\lambda_{\text{tar}}$ is set at 8 pm, corresponding to a photon energy of 155 keV in the $\gamma$-ray regime. In the FEL, the fundamental resonant wavelength is given by [21]

$$\lambda_{\text{res}} = \frac{\lambda_u}{2\gamma^2}\left(1 + \frac{K^2}{2}\right).$$

For the given values of $\gamma$ and $\lambda_u$, there is no positive real value of $K$ for which $\lambda_{\text{res}} = \lambda_{\text{tar}}$, so harmonic lasing is the only way to reach $\lambda_{\text{tar}}$. Once $\lambda_{\text{res}}$ is set, harmonic lasing enables access to shorter wavelengths of the form $\lambda_{\text{res}}/h$, where $h$ is a harmonic number. Along the undulator axis, only the odd harmonics $h \in \{1, 3, 5, \dots\}$ are present.

ISBN: 978-3-95450-248-6 ISSN: 2673-5490 doi: 10.18429/JACoW-IPAC2025-MOPB035

### *The FEL Schemes*

The three FEL schemes considered here for the purpose of harmonic lasing are (i) conventional SASE, (ii) the phase shifter scheme and (iii) the split-undulator scheme.

For conventional SASE, a constant value of $K = 1.64$ is used throughout. This value approximates the minimum feasible $K$ for the SASE1 line of the European XFEL [20]. It produces a resonant wavelength of $\lambda_{\mathrm{res}} = 40\,\mathrm{pm}$, equivalent to a photon energy of 31 keV in the hard x-ray regime. The target wavelength corresponds to the fifth harmonic of the resonant wavelength, expressed as $\lambda_{\mathrm{tar}} = \lambda_{\mathrm{res}}/h$ with $h = 5$. All phase shifters are configured to $\phi = 0$, preserving the phase angle between the electron bunch and the radiation pulse across each drift section.

In the phase shifter scheme, all settings are identical to those of conventional SASE, except that $\phi$ is set to different integer multiples of $\phi(\lambda_{\mathrm{tar}})$ in different drift sections, where $\phi(\lambda_{\mathrm{tar}}) = 2\pi \times \lambda_{\mathrm{tar}}/\lambda_{\mathrm{res}} = 2\pi/5$.

In the split-undulator scheme, the undulator segments are allocated into two sections. The first section is configured identically to conventional SASE. The second section is set to a different $K$ value, resulting in a new resonant wavelength $\lambda'_{\mathrm{res}}$. Consequently, the same target wavelength $\lambda_{\mathrm{tar}}$ corresponds to a different harmonic number $h'$ of this new resonant wavelength $\lambda'_{\mathrm{res}}$, such that $\lambda_{\mathrm{tar}} = \lambda_{\mathrm{res}}/h = \lambda'_{\mathrm{res}}/h'$ with $h' \neq h$. All phase shifters are set to $\phi = 0$.

## RESULTS

The simulation results are shown in Fig. 1, with the three columns representing conventional SASE, the phase shifter scheme and the split-undulator schemes, respectively.

The first row depicts the undulator and phase shifter configurations along the FEL line. For the split-undulator scheme [see Fig. 1(c)], the harmonic number $h'$ in the second section and the allocation of undulator segments between sections are optimised parameters. Optimal values of $h' = 11$ and an undulator segment ratio of $16 : 20$ between the two sections were selected.

The second row presents the brightness $B_h$ as a function of position $z$ for harmonic numbers $h = 1, 3, 5$. For the split-undulator scheme [see Fig. 1(f)], these harmonic numbers correspond to those for the resonant wavelength $\lambda_{\mathrm{res}}$ of the first section, as opposed to $\lambda'_{\mathrm{res}}$ of the second section. Harmonics higher than the target harmonic ($h = 5$) are excluded here, as they are found to be orders of magnitude lower in brightness at the end of the FEL line across all three schemes, thus rendering them less significant.

In conventional SASE [see Fig. 1(d)], there is an inverse correlation between harmonic number and maximum brightness, with the fundamental mode ($h = 1$) being dominant, consistent with expectations. In contrast, the phase shifter scheme [see Fig. 1(e)] suppresses the unwanted harmonics ($h = 1$ and $h = 3$), keeping their brightness below that at the target harmonic ($h = 5$) over much of the FEL line. However, a comparison of the red curves in Figs. 1(d) and (e) reveals that the phase shifter scheme delays the growth and saturation of brightness at the target harmonic. Consequently, the phase shifter scheme yields a lower final brightness compared to conventional SASE.

In the split-undulator scheme [see Fig. 1(f)], the boundary at $z = 97.6\,\mathrm{m}$ demarcates the two sections. Prior to this point, the brightness curves resemble those of conventional SASE [see Fig. 1(d)]. Beyond the boundary, the brightness of the unwanted harmonics ($h = 1$ and $h = 3$) decreases gradually, due to two combined effects: (i) the radiation power ceases to grow and stays constant; (ii) diffraction widens the beam radius (data not shown). In contrast, the target harmonic ($h = 5$) exhibits sustained growth and its final brightness exceeds that in both other schemes [see Figs. 1(d) and (e)].

The bottom row in Fig. 1 displays the SNR as a function of $z$, with a horizontal dashed line marking unity for visual guidance. Here, the SNR is defined as $B_5/(B_1 + B_3)$. For conventional SASE, the SNR remains below one throughout the FEL line. The phase shifter scheme marginally enhances performance over conventional SASE, achieving an SNR above unity in the latter section of the FEL line. The split-undulator scheme exhibits a sharp, significant increase in SNR beyond the boundary at $z = 97.6\,\mathrm{m}$, resulting in a substantially higher SNR compared to the other schemes.

From the perspective of the FEL user at the experimental station, the final parameters at the end of the FEL line are critical. These parameters are presented in Table 2. Regarding the final SNR, the split-undulator scheme outperforms the phase shifter scheme by over a hundredfold and achieves more than a thousandfold improvement over conventional SASE. In terms of the final brightness $B_5$ at the target harmonic, the phase shifter scheme underperforms compared to conventional SASE, exhibiting a brightness reduction of 3%. Conversely, the split-undulator scheme surpasses conventional SASE by almost an order of magnitude.

Table 2: Simulation results for the end of the FEL line. The top rows show the final brightness $B_h$ in units of photons $\mathrm{s}^{-1}$ $\mathrm{mm}^{-2}$ $\mathrm{mrad}^{-2}$ $(0.1\%\ \mathrm{bandwidth})^{-1}$ for harmonic numbers $h = 1, 3, 5$ of the wavelength $\lambda_{\mathrm{res}}$. The bottom row reports the corresponding SNR, defined here as $B_5/(B_1 + B_3)$.

| | Conventional SASE | Phase Shifter Scheme | Split-Undulator |
|---|---|---|---|
| $B_1$ | $4.1 \times 10^{31}$ | $3.4 \times 10^{28}$ | $7.2 \times 10^{28}$ |
| $B_3$ | $7.3 \times 10^{30}$ | $3.0 \times 10^{29}$ | $2.6 \times 10^{28}$ |
| $B_5$ | $6.6 \times 10^{30}$ | $8.3 \times 10^{29}$ | $2.8 \times 10^{31}$ |
| SNR | 0.14 | 2.5 | 290 |

## DISCUSSION

The simulation results highlight the superb performance of the novel split-undulator scheme, evaluated through two key figures of merit at the end of the FEL line: (i) the brightness at the target harmonic and (ii) the SNR.

The efficacy of the scheme stems from the target wavelength being a harmonic of both $\lambda_{\mathrm{res}}$ and $\lambda'_{\mathrm{res}}$, enabling its

ISBN: 978-3-95450-248-6 ISSN: 2673-5490 doi: 10.18429/JACoW-IPAC2025-MOPB035



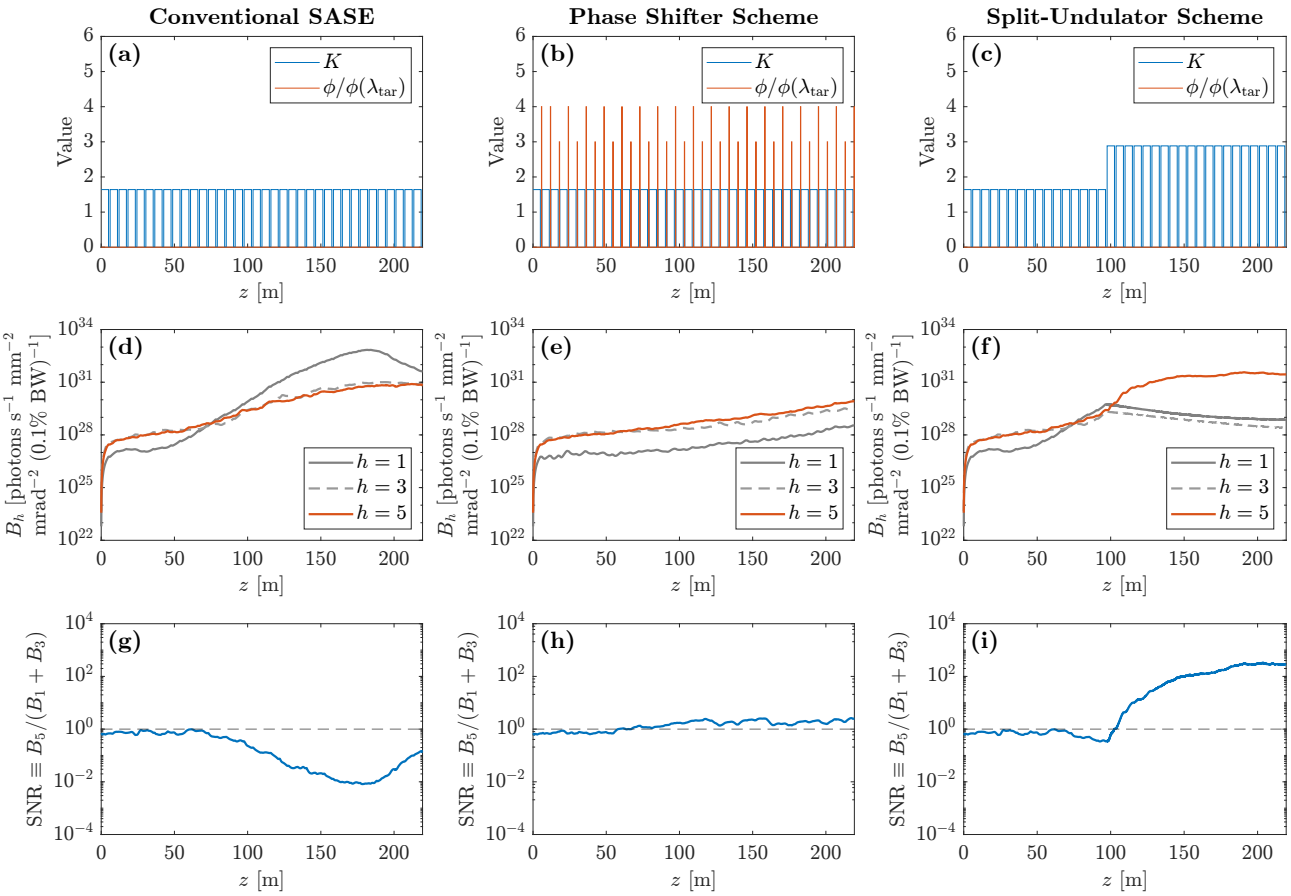


Figure 1: Simulation results. The three columns represent the three FEL schemes: conventional SASE (left), the phase shifter scheme (centre) and the split-undulator scheme (right). The top row illustrates the undulator and phase shifter configurations along the FEL line. The middle row displays the brightness $B_h$ as a function of the distance $z$ along the FEL line for harmonic numbers $h = 1, 3, 5$ of the wavelength $\lambda_{\mathrm{res}}$. The bottom row shows the SNR as a function of $z$, defined in this context as $B_5/(B_1 + B_3)$.

amplification in both sections of the FEL line. In contrast, unwanted harmonics of $\lambda_{\mathrm{res}}$ in the first section are generally not amplified in the second section, allowing energy to be redirected to the target wavelength in accordance with the principle of energy conservation.

However, the simulations have limitations. In the default simulation mode of GENESIS [18], a single reference wavelength applies across the entire FEL line. When simulating the split-undulator scheme, the resonant wavelength $\lambda_{\mathrm{res}}$ of the first section serves as the reference wavelength. Consequently, radiation properties at the resonant wavelength $\lambda'_{\mathrm{res}}$ of the second section and its harmonics are not computed.

In principle, electrons could develop microbunching at intervals of $\lambda'_{\mathrm{res}}$ as they traverse the second section, potentially increasing the brightness at the unwanted harmonics of $\lambda'_{\mathrm{res}}$. These harmonics contribute to noise, which should be accounted for in the SNR. To address this, further exploration of advanced simulation modes in GENESIS or the use of alternative simulation codes, such as Puffin [22], may be necessary. These investigations are ongoing.

If the unwanted harmonics of $\lambda'_{\mathrm{res}}$ prove to be substantial in brightness, they could be suppressed using appropriate phase shifts, thereby combining the features of the split-undulator and phase shifter schemes. This could be a subject for further exploration.

## CONCLUSION

An innovative split-undulator scheme has been proposed to extend the spectral reach of existing FELs into the $\gamma$-ray regime through harmonic lasing. Simulations indicate superior performance compared to the pre-existing phase shifter scheme in terms of brightness and SNR. Although the simulations have limitations which warrant further investigation, this work represents a key step towards the $\gamma$-ray free-electron laser ($\gamma$FEL), or free-electron graser (FEG).

## REFERENCES

[1] W. Decking *et al.*, "A MHz-repetition-rate hard X-ray free-electron laser driven by a superconducting linear accelerator", *Nature Photonics*, vol. 14, no. 6, pp. 391–397, 2020. doi:10.1038/s41566-020-0607-z

[2] C. Bostedt *et al.*, "Linac Coherent Light Source: The first five years", *Reviews of Modern Physics*, vol. 88, no. 1, p. 015 007, 2016. doi:10.1103/revmodphys.88.015007

ISBN: 978-3-95450-248-6 ISSN: 2673-5490 doi: 10.18429/JACoW-IPAC2025-MOPB035

[3] I. Eom *et al.*, "Recent progress of the PAL-XFEL", *Applied Sciences*, vol. 12, no. 3, p. 1010, 2022. doi:10.3390/app12031010

[4] M. Yabashi, H. Tanaka, K. Tono, and T. Ishikawa, "Status of the SACLA facility", *Applied Sciences*, vol. 7, no. 6, p. 604, 2017. doi:10.3390/app7060604

[5] C. Milne *et al.*, "SwissFEL: The Swiss x-ray free electron laser", *Applied Sciences*, vol. 7, no. 7, p. 720, 2017. doi:10.3390/app7070720

[6] E. A. Seddon *et al.*, "Short-wavelength free-electron laser sources and science: A review", *Reports on Progress in Physics*, vol. 80, no. 11, p. 115 901, 2017. doi:10.1088/1361-6633/aa7cca

[7] C. Callegari, A. N. Grum-Grzhimailo, K. L. Ishikawa, K. C. Prince, G. Sansone, and K. Ueda, "Atomic, molecular and optical physics applications of longitudinally coherent and narrow bandwidth free-electron lasers", *Physics Reports*, vol. 904, pp. 1–59, 2021. doi:10.1016/j.physrep.2020.12.002

[8] J. F. Ong, M.-H. Koh, and I. H. Hashim, "Nuclear photonics: Laser-driven nuclear physics", *IOP Conference Series: Materials Science and Engineering*, vol. 1285, no. 1, p. 012 003, 2023. doi:10.1088/1757-899x/1285/1/012003

[9] D. L. Balabanski and W. Luo, "Nuclear photonics and nuclear isomers", *The European Physical Journal Special Topics*, vol. 233, no. 5, pp. 1161–1179, 2024. doi:10.1140/epjs/s11734-024-01132-3

[10] V. L. Ginzburg, "Nobel Lecture: On superconductivity and superfluidity (what I have and have not managed to do) as well as on the "physical minimum" at the beginning of the XXI century", *Reviews of Modern Physics*, vol. 76, no. 3, pp. 981–998, 2004. doi:10.1103/revmodphys.76.981

[11] B. W. J. McNeil, G. R. M. Robb, M. W. Poole, and N. R. Thompson, "Harmonic lasing in a free-electron-laser amplifier", *Physical Review Letters*, vol. 96, no. 8, p. 084 801, 2006. doi:10.1103/physrevlett.96.084801

[12] E. A. Schneidmiller and M. V. Yurkov, "Harmonic lasing in x-ray free electron lasers", *Physical Review Special Topics - Accelerators and Beams*, vol. 15, no. 8, p. 080 702, 2012. doi:10.1103/physrevstab.15.080702

[13] L.-H. Yu *et al.*, "High-gain harmonic-generation free-electron laser", *Science*, vol. 289, no. 5481, pp. 932–934, 2000. doi:10.1126/science.289.5481.932

[14] D. Xiang and G. Stupakov, "Echo-enabled harmonic generation free electron laser", *Physical Review Special Topics - Accelerators and Beams*, vol. 12, no. 3, p. 030 702, 2009. doi:10.1103/physrevstab.12.030702

[15] C. Feng, H. Deng, D. Wang, and Z. Zhao, "Phase-merging enhanced harmonic generation free-electron laser", *New Journal of Physics*, vol. 16, no. 4, p. 043 021, 2014. doi:10.1088/1367-2630/16/4/043021

[16] E. Schneidmiller *et al.*, "First operation of a harmonic lasing self-seeded free electron laser", *Physical Review Accelerators and Beams*, vol. 20, no. 2, p. 020 705, 2017. doi:10.1103/physrevaccelbeams.20.020705

[17] D. Dunning *et al.*, "The UK XFEL conceptual design and options analysis: Mid-term update", in *Proceedings of the 15th International Particle Accelerator Conference*, Nashville, TN, USA, May 2024, pp. 400–403. doi:10.18429/JACoW-IPAC2024-MOPG55

[18] S. Reiche, "GENESIS 1.3: A fully 3D time-dependent FEL simulation code", *Nuclear Instruments and Methods in Physics Research Section A*, vol. 429, no. 1–3, pp. 243–248, 1999. doi:10.1016/s0168-9002(99)00114-x

[19] E. Schneidmiller and M. Yurkov, "Baseline parameters of the European XFEL", in *Proceedings of the 38th International Free Electron Laser Conference*, Santa Fe, NM, USA, Aug. 2017, pp. 109–112. doi:10.18429/JACoW-FEL2017-MOP033

[20] S. Abeghyan *et al.*, "First operation of the SASE1 undulator system of the European X-ray Free-Electron Laser", *Journal of Synchrotron Radiation*, vol. 26, no. 2, pp. 302–310, 2019. doi:10.1107/s1600577518017125

[21] Z. Huang and K.-J. Kim, "Review of x-ray free-electron laser theory", *Physical Review Special Topics - Accelerators and Beams*, vol. 10, no. 3, p. 034 801, 2007. doi:10.1103/physrevstab.10.034801

[22] L. T. Campbell and B. W. J. McNeil, "Puffin: A three dimensional, unaveraged free electron laser simulation code", *Physics of Plasmas*, vol. 19, no. 9, p. 093 119, 2012. doi:10.1063/1.4752743